PERSPECTIVE

Topology-Aided Molecular Design: The Platonic Molecules of Genera 0 to 3

Erwin Lijnen* and Arnout Ceulemans

Departement Chemie, K.U. Leuven, Celestijnenlaan 200F, B-3001 Leuven, Belgium

Received June 20, 2005

1. INTRODUCTION

Symmetry plays an important role as a guiding principle for the design of novel molecules.[1] The fascination for symmetrical molecular architectures in three dimensions can be traced back to van't Hoffs bold hypothesis of tetrahedral carbon and knew glorious moments in the last century with the successful synthesis of the icosahedral closo-borane[2] and of dodecahedrane[3] and last but not least with the unexpected self-assembly of the truncated icosahedral buckminsterfullerene cage from a cooling carbon plasma.[4]

The icosahedron is the largest member of the point group family, and thus the highest symmetry group that can be attained in three dimensions. From here on chemistry must use new guiding principles in its quest for novel structures. For such a deeper principle we turn to topology. The basic objects of topology are two-dimensional closed surfaces. The topological feature which distinguishes these surfaces is their genus. This is nothing else than the number of holes going through the surface. In this article we discuss the complete list of regular surface networks that cover topologies with genera from 0 to 3.

The chemical literature already contains a number of inspiring links to mathematical developments. We especially mention the works of King[5,6] and of Mackay and Terrones.[7] Our aim is to bring these results home in a general framework and elaborate the molecular realization on a rigorous symmetry basis. Most of the resulting structures have not been synthesized yet and might constitute interesting targets for a topology-aided chemical design.[8−11] Mathematical aspects have been derived before in a set of specialized papers.[12−16] Here we collect these results in a complete overview and put emphasis on the pictorial representations of these structures.

2. FROM GRAPH TO MAP

In real life, a molecule consists of some positively charged atomic nuclei held together by a cloud of negatively charged electrons. In most applications this picture is simplified, and a molecule is represented as a set of beads held together by strings. In mathematics, this representation corresponds to a graph[17] where the vertices (points) denote the atoms of the molecule and the edges (lines) correspond to bonds. This graphlike model is purely combinatorial in nature, meaning it is freed from all spatial information. Although this graphlike representation has been proven useful for the qualitative description of a multitude of chemical problems,[18] its complete lack of spatial information can sometimes be disadvantageous. In these instances one would prefer a more elaborate representation which also contains some of the 3D information of the actual physical structure. The first and most elementary way to add some geometrical information to this graphlike model is by mapping the graph on a 2D closed surface like the sphere or the torus to form a *2-cell embedding* or *map*.[13,19] When such a mapping takes place, the graph covers the underlying surface by a set of 2D closed regions which are called *2-cells* or *faces*. Aside from vertices and edges, this new type of structural element introduces spatial information into the model. A further development would imply a *3-cell embedding* where the molecule is further divided in chambers. In this paper we will not consider this extension and limit ourselves to molecular networks that can be mapped on surfaces.[20]

For maps on orientable surfaces, the topology of the underlying surface and the number of vertices, edges, and faces are related by the celebrated Euler theorem which states

$$V - E + F = 2 - 2g \tag{1}$$

where V, E, and F denote the number of vertices, edges, and faces of the map, and g denotes the genus of the map which is nothing else than the number of holes in the underlying surface.

In the present paper we will not be concerned with just any map but will limit ourselves to the *regular maps*.[21−23] Such maps reveal the basic structure of the surface. Irregular structures can always be characterized as distortions of the regular ones. The term "regular map" originates from mathematics and may not be familiar to the general reader. It is a collective name for those maps which exhibit the highest possible degree of symmetry. For the surface of genus zero (the sphere) these regular maps can be identified with the well-known Platonic solids. In the following we will extent this term to all genera and call them Platonics.

A symmetry operation of a map is a permutation of its vertices which keeps the incidence relations on the vertices as well as on the edges and the faces. A Platonic is defined as a map where the symmetry group acts transitively on all three sets of structural elements (vertices, edges, and faces). This implies that all faces as well as all edges and all vertices are equivalent. To satisfy this condition the order of the symmetry group should at least equal twice the number of edges (2E), in which case one speaks of *chiral* Platonics.

* Corresponding author fax: +32 16 32 79 92; e-mail: erwin.lijnen@chem.kuleuven.be.

10.1021/ci0502496 CCC: $30.25
Published on Web 10/19/2005

Table 1. Platonics of Genus 0

Schläfli	vertices	edges	faces	group	group order	name
{3,3}	4	6	4	T_d	24	tetrahedron
{4,3}	8	12	6	O_h	48	cube
{3,4}	6	12	8	O_h	48	octahedron
{5,3}	20	30	12	I_h	120	dodecahedron
{3,5}	12	30	20	I_h	120	icosahedron
{2,*k*}	2	k	k	D_{kh}	4*k*	k-gonal hosohedron
{*k*,2}	k	k	2	D_{kh}	4*k*	k-gonal dihedron

However, most Platonics have a higher symmetry as they also contain reflectional symmetry. In this case the order of the symmetry group equals four times the number of edges (4E). They are called *reflexible* Platonics and indeed attain the highest symmetry which is possible for a map.[21]

In the following sections all regular maps of genus 0 to 3 (from the sphere to the triple torus) will be identified. In all cases, an analogy is made with some already existing molecules or with chemical structures that are still purely hypothetical in nature but can form some serious challenges for the synthetic chemist.

3. PLATONICS OF GENUS 0

The Platonics of genus 0, that can be mapped on the surface of a sphere, have a long history and can be traced back to the ancient Greeks, who thought they could be identified with the four elementals and the universe. In Table 1 we give a list of the Platonics together with some of their main properties. For mathematical completeness we also included the k-gonal hosohedron formed by connecting two antipodal vertices on the sphere by *k* edges and the k-gonal dihedron formed by a ring of *k* vertices around the equator of the sphere and thereby dividing it into two hemispheres. If we identify vertices with atoms and edges with chemical bonds, the former will reduce to a pair of atoms connected by *k* different bonds and the latter just corresponds to a cycle of *k* atoms. They are therefore excluded from further discussion. The five remaining spherical Platonics are the ones we are familiar with, namely the tetrahedron, the cube, the octahedron, the dodecahedron, and the icosahedron. In the table they are identified by their Schläfli notation $\{p, q\}$ where the first entry *p* denotes the face-sizes and the second entry *q* corresponds with the vertex degrees. Inspection of the table reveals three pairs which share a common symmetry group, namely the cube−octahedron pair with octahedral O_h symmetry, the dodecahedron−icosahedron pair with icosahedral I_h symmetry and the hosohedron−dihedron pair with dihedral D_{kh} symmetry. The Platonics within such a pair are related by Poincaré duality. A Poincaré dual of a map can be formed by identifying the vertices of the new map with the face-centers of the original map and only connecting those vertices for which the corresponding faces were adjacent in the original structure. It can be shown that within such a dual pair the numbers of vertices and faces are interchanged where the number of edges stays unaltered. During this dualization process genus and symmetry are preserved, but the decorating graph is changed. As a result, for a given genus, all Platonics should appear in pairs unless, like the tetrahedron, they are self-dual.

The aesthetics and extremely high symmetry of these structures has stimulated the chemical community to search for molecular realizations. This has led, especially during the past decades, to the synthesis of a multitude of clusters resembling these Platonics. The best known examples for the trivalent cases (tetrahedron, cube, and dodecahedron) are probably the carbohedranes: tetrahedrane (C_4H_4), cubane (C_8H_8), and dodecahedrane ($C_{20}H_{20}$). Tetrahedrane consists of four carbon atoms which are arranged at the corners of a tetrahedron together with four outward pointing exopolyhedral hydrogen atoms. This tetrahedral skeleton is characterized by a considerable strain which can be substantially reduced by a substitution of the hydrogen atoms with more voluminous substituents.[24] For cubane the carbon atoms occupy the corners of a cube.[25] Especially the nitro-derivative $C_8(NO_2)_8$ currently receives a lot of attention as it is highly explosive but shock-resistant.[26] Dodecahedrane (Figure 1) forms the last member of this carbohedrane series, and recently even claims have been made about the existence of pure carbon C_{20} clusters in the gas phase.[27] The two remaining structures (octahedron and icosahedron) are characterized by higher valencies and trigonal faces and can be realized by the members $B_6H_6^{2-}$ and $B_{12}H_{12}^{2-}$ (Figure 1) of the electron-deficient closo-borane series.[2,28] Aside from these carbon and boron based structures, the inorganic chemist will be familiar with a multitude of other structures such as the metallo-carbohedrenes (for example the dodecahedral Ti_8C_{12} cluster[29]) or the hexanuclear Mo, W, Nb, or Ta clusters.[30]

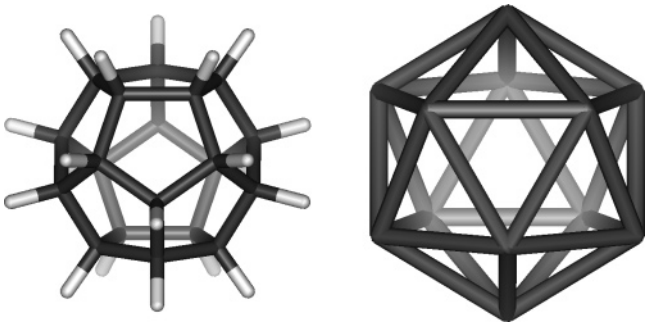

Figure 1. Realizations of the dodecahedral carbohedrane $C_{20}H_{20}$ (left) and the icosahedral closo-borane $B_{12}H_{12}^{2-}$ (right).

Table 2. Platonics of Genus 1[a]

tessellation	Schläfli	vertices	edges	faces	group order
triangular	$\{3,6\}_{n,m}$	$\sigma/2$	3σ	3σ	6σ
	$\{3,6\}_{n,0}$	n^2	$3n^2$	$2n^2$	$12n^2$
	$\{3,6\}_{n,n}$	$3n^2$	$9n^2$	$6n^2$	$36n^2$
quadrangular	$\{4,4\}_{n,m}$	ϵ	2ϵ	ϵ	4ϵ
	$\{4,4\}_{n,0}$	n^2	$2n^2$	n^2	$8n^2$
	$\{4,4\}_{n,n}$	$2n^2$	$4n^2$	$2n^2$	$16n^2$
hexagonal	$\{6,3\}_{n,m}$	2σ	3σ	$\sigma/2$	6σ
	$\{6,3\}_{n,0}$	$2n^2$	$3n^2$	n^2	$12n^2$
	$\{6,3\}_{n,n}$	$6n^2$	$9n^2$	$3n^2$	$36n^2$

[a] $\sigma = n^2 + nm + m^2$ / $\epsilon = n^2 + m^2$.

4. PLATONICS OF GENUS 1

The surface of genus 1 corresponds to a torus. There exists an infinite number of toroidal Platonics,[22] which fall into three general families. Table 2 gives an overview of these three families together with some properties. The symmetry groups of the maps can be found in the specialized mathematical literature.[23] We limit ourselves here to listing their orders.

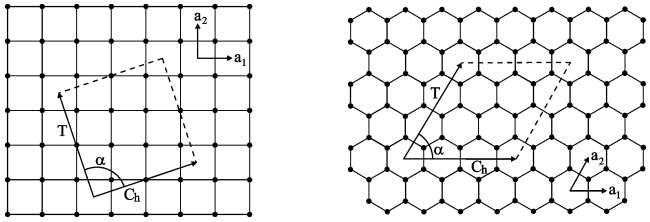

Figure 2. Identification of a patch on the plane which is regularly tessellated by squares (left) and hexagons (right). The chiral vectors $\mathbf{C_h}$ and twist vectors $\mathbf{T}$ have been chosen in a way that the patches form regular tori.

A torus can be constructed by cutting a parallelogram out of the plane and identifying its opposite edges. Figure 2 shows such parallelograms which are extracted from a square and hexagonally tessellated plane. The parallelogram is spanned by two vectors: a chiral vector $\mathbf{C_h}$ and a twist vector $\mathbf{T}$, which subtend an angle α. The only restriction imposed on these vectors is that they start from a common point and that they connect symmetry equivalent points on the lattice. Both vectors can thus be expressed by integer multiples of the translational unit vectors $\mathbf{a_1}$ and $\mathbf{a_2}$:

$$\mathbf{C_h} = n\mathbf{a_1} + m\mathbf{a_2} \tag{2}$$

$$\mathbf{T} = p\mathbf{a_1} + q\mathbf{a_2} \tag{3}$$

Out of this patch a tubelike structure can be constructed by identifying a first set of parallel edges. By convention one first identifies the points which are brought to each other by the chiral vector $\mathbf{C_h}$, meaning that the chiral vector will be wound around the tube. In the case of the hexagonal lattice, this newly formed tubelike structure exactly corresponds with a finite carbon nanotube.[31] In a second step we can identify the two boundaries of the tube by identifying the points which are brought together by the twist vector $\mathbf{T}$. In this way the nanotube closes to form a carbon nanotorus. The twist vector $\mathbf{T}$ now runs along the spine of the torus and is always chosen in the 180° wedge of the lattice counterclockwise from $\mathbf{C_h}$ to $-\mathbf{C_h}$, thus $0 \leq \alpha < \pi$. Using this formalism, it is possible to describe every hexagonally tessellated torus by two vectors $\mathbf{C_h} = (n, m)$ and $\mathbf{T} = (p, q)$ or simply by a 4-tuple of integers (n, m, p, q).[32]

As the plane can only be regularly tessellated by triangles, squares, or hexagons, the same holds true for a torus. It is however not so that every torus formed from these planes will necessarily form a regular map of genus one. In fact, to form a regular torus, some further constraints should be imposed on the $\mathbf{C_h}$ and $\mathbf{T}$ vectors. Let us start with the example of the {4,4} tori formed from a tessellation of the plane by squares. Figure 2a shows a patch of this plane together with its two translational unit vectors which in this case make an angle of $\pi/2$. It is only when the $\mathbf{C_h}$ and $\mathbf{T}$ vectors have an equal length and span an angle $\alpha = \pi/2$, that the corresponding torus will be Platonic. This explains the notation in Table 2 where each squarely tessellated regular toroidal map is only described by the set of integers (n, m) defining its $\mathbf{C_h}$ vector as this automatically fixes the set of integers specifying the $\mathbf{T}$ vector to be $(-m, n)$.

Because of the 4-fold rotational symmetry of the planar {4,4} tessellation the $\mathbf{C_h}$ vector can always be rotated by multiples of $\pi/2$ to form a new $\mathbf{C_h}$ vector with $n, m \geq 0$,

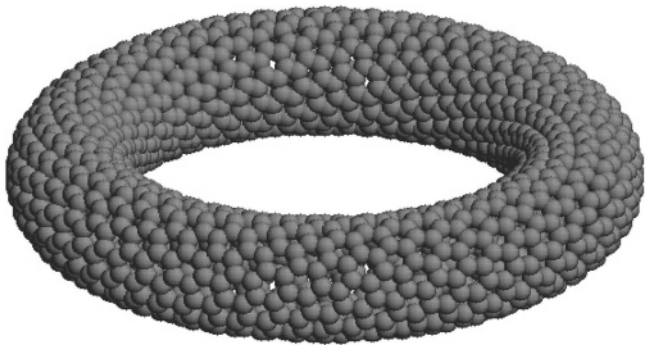

Figure 3. The hexagonal torus (4, 10, − 64, 48) with D_{16} symmetry (taken from ref 33).

which describes exactly the same torus. The $\mathbf{C_h}$ vector can therefore be restricted to the quadrant where $n > 0$ and $m \geq 0$. (In case one of the coordinates is zero, $(n, 0)$ is preferred over $(0, n)$). In general all Platonic tori formed by this procedure will be chiral. Only when $n = m$ or $m = 0$ these maps will also exhibit reflectional symmetry and therefore form reflexible Platonics.

The cases $\{6,3\}_{n,m}$ and $\{3,6\}_{n,m}$ can be described in a similar way. We will limit ourselves to the case of the hexagonal tori as all triangular tori are related by Poincaré duality. As depicted in Figure 2b we can choose the translational unit vectors in such a way that they make an angle of $\pi/3$. In this case all Platonics are described by a random chiral vector $\mathbf{C_h} = (n, m)$ (with $n > 0$ and $m \geq 0$ because of the 6-fold symmetry) together with a twist vector $\mathbf{T} = (-m, n + m)$ of equal length which is rotated over an angle $\pi/3$ or a twist vector $\mathbf{T} = (-n - m, n)$ of equal length rotated over an angle of $2\pi/3$. The condition for reflexibility is again that $m = n$ or $m = 0$, corresponding to armchair and zigzag, respectively.

The most interesting tori are certainly the ones that are tessellated by hexagons as they are easily identified with carbon nanotori. Although the physical properties of these tori are well investigated,[32,33] their actual synthesis is still an open question. Small tori are necessarily excluded as their dimensions are not large enough to cope with the strain which results from bending the patch to a tube and then to a torus. Molecular realizations of regular carbon nanotori are also excluded. Indeed for all regular tori the chiral vector and twist vector should be of equal length. This imposes a serious problem for their 3D realization as the exact one-to-one ratio leads to tori with tubes which are so thick that the central hole of the torus is completely shrunk to a single point. It is therefore impossible to realize these regular tori in 3D space. Nonetheless while the high permutational symmetries of the genus 1 Platonics are outside molecular reach, by a careful choice of the coordinates of the chiral and twist vectors it may be possible to attain some quite large symmetries for nonregular tori. As a fictitious example, in Figure 3 we show the torus (4, 10, − 64, 48) which exhibits D_{16} symmetry. Chemical realizations of tori which are tessellated by triangles or squares deal with the same sort of problems and are even more hypothetical than their carbon analogues. One could think of triangular tori with their backbone formed by boron atoms or squarely tessellated tori consisting of atoms, like Pt, which can form square-planar coordinations.

Table 3. Platonics of Genus 2[a]

Schläfli	vertices	edges	faces	group order
{8,3}	16	24	6	96
{6,4}	6	12	4	48
{8,4}	4	8	2	32
{10,5}	2	5	1	20
{6,6}	2	6	2	24
{8,8}	1	4	1	16

[a] For maps related by Poincaré duality we only list the member with the largest face size and lowest vertex degree (taken from ref 21).

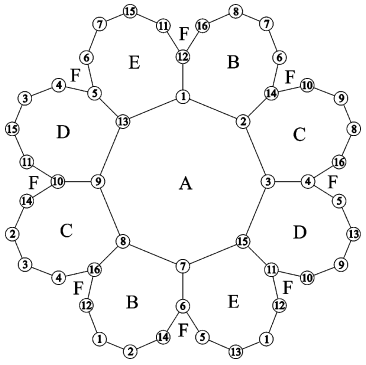

Figure 4. Schlegel-like representation of the genus-2 Möbius-Kantor map on 16 vertices. The map consists of 6 octagonal faces which are indicated by the letters A to F.

5. PLATONICS OF GENUS 2

When we go one step further to consider molecular realizations of genus 2 Platonics, we find ourselves on completely new and unexplored territory. A genus 2 surface is also called a double torus or pretzel. Table 3 gives the list of the regular maps of genus 2, where for those maps which are related by Poincaré duality, we only listed the member with the largest face size and lowest vertex degree. Some of the listed maps only obey the Platonicity condition because their vertices are connected by multiple edges. In these cases, the maps showing the actual connectivity of the network (maps where all multiple bonds are replaced by single bonds) will be of much lower symmetry. We will therefore exclude them from further discussion and only investigate those maps which achieve their Platonicity conditions by means of single edges. For genus 2 this reduces the list to the single map with Schläfli notation {8,3}. (All other maps and their Poincaré duals are characterized by multiple bonds.) We will call this map the genus two Möbius-Kantor map as its underlying graph is the highly symmetrical Möbius-Kantor graph on 16 vertices. Such a higher genus map can most easily be visualized by a Schlegel-like projection in the plane (Figure 4). By identifying vertices and edges which repeat themselves along the outer boundary, the original map on the double torus can easily be reconstructed. One should however note that because of the low number of vertices in this structure, the corresponding spatial realization on the double torus will be much too strained to be chemically plausible. However, as in the previous case of the genus-1 surface, instead of mapping a graph on a closed double torus, we may choose an open surface which is periodic in two directions and forms a 2D equivalent of the well-known plumber's nightmare surface (Figure 5). By replacing cyclic boundaries by periodic boundaries the graph connectivity is kept. Of course, we are

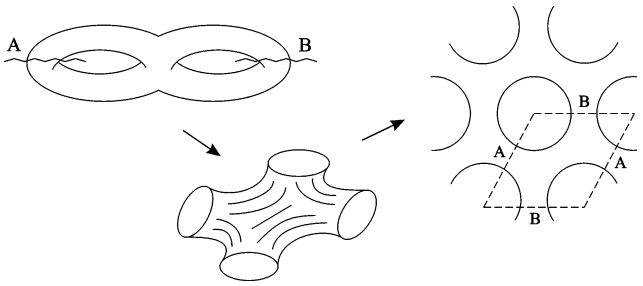

Figure 5. Opening of the double torus or pretzel to form the 2D equivalent of the plumber's nightmare. The resulting structure can serve as the unit-cell (dashed lines) of a hexagonal tubular lattice exhibiting D_{6h} symmetry.

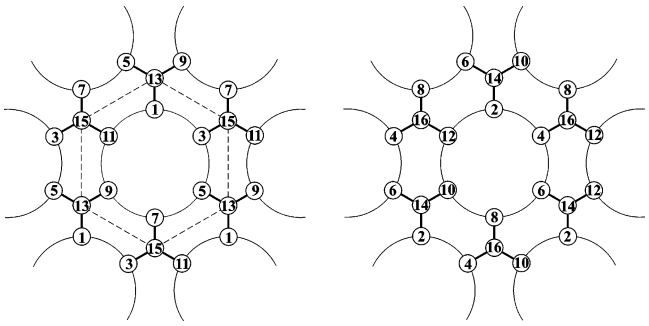

Figure 6. Embedding of the regular genus-2 map of the MK-graph on a surface with D_6 symmetry viewed along the C_6 axis. (Left: top view / right: bottom view).

interested in finding the highest symmetrical realization so the choice of the underlying periodic surface will be of primordial importance as the symmetry of the 3D realization of the map can never exceed the symmetry of the surface on which it is embedded. Our strategy to find the appropriate structure was based on the observation that the automorphism group of the Möbius-Kantor map contains a D_6 point group which matches the symmetry of the hexagonal tubular lattice.

The positioning of the vertices and edges on this surface is guided by the structure of the vertex and edge orbits under the D_6 subgroup. Under this symmetry, the vertices split into two orbits: one of length 12 (vertices 1 to 12) and one of length 4 (vertices 13−16). The first orbit therefore corresponds with a vertex in a general position together with all its images under D_6 symmetry. Here we have chosen to put these vertices around the central hole of the hexagonal unit cell. As the second orbit only consists of four vertices they must occupy a special position namely the corners of the hexagonal unit-cell. Notice that of the twelve corners only four are nonequivalent. The placement of the vertices is illustrated in Figure 6 where we give a top view (left) and bottom view (right) of the tubular system. In a similar way the edges can be partitioned into three orbits, one of length 12 and two of length 6. The largest orbit just connects the atoms which are lying around the central hole to the atoms on the corners. The other two orbits cannot be visualized in Figure 6 as they lie on the inside of the central hole and make connections between atoms on the upper and lower part of the unit-cell. Of these orbits there is one which connects vertices which are lying directly above each other like edge (1−2). The remaining orbit makes connections such as the edge (2−3). Out of the schematic pictures of Figure 6 we constructed a molecular model by replacing the vertices with carbon atoms. The resulting structures were optimized

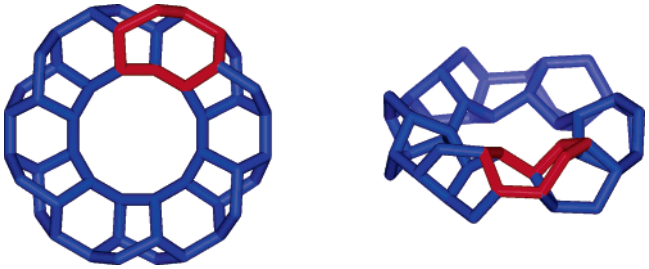

Figure 7. Top view (left) and side view (right) of the all-octagon carbon network based on the genus-2 Möbius-Kantor map. One of the octagonal faces is indicated in blue.

Table 4. Platonics of Genus 3[a]

Schläfli	vertices	edges	faces	group order	name
{7,3}	56	84	24	336	Klein
{8,3}	32	48	12	192	Dyck
{12,3}	16	24	4	96	Möbius-Kantor
{6,4}	12	24	8	96	
{8,4}	8	16	4	64	
{8,4}	8	16	4	64	
{12,4}	6	12	2	48	
{6,6}	4	12	4	48	
{8,8}	2	8	2	32	
{8,8}	2	8	2	32	
{14,7}	2	7	1	28	
{12,12}	1	6	1	24	

[a] For maps related by Poincaré duality we only list the member with the largest face size and lowest vertex degree (taken from ref 21).

using MM+ molecular modeling and are shown in Figure 7. Notice that just like the schematic pictures, they show a little bit more than one hexagonal unit-cell. One of the faces has been given a blue color to emphasize that the surface is indeed tessellated by octagons and corresponds with the genus-2 Möbius-Kantor map. Using this structure as a building block, a carbon network can be formed that propagates in two dimensions and which forms a first realization of a Platonic on a higher genus surface than the torus.

6. PLATONICS OF GENUS 3

A closed surface of genus 3 is a triple torus or a sphere with three handles. Equivalently this genus can be realized as a 3D periodic lattice, known as the plumber's nightmare.[5] In Table 4 we identify the regular maps of genus 3 where once again for each pair of Poincaré duals only the member with the lowest vertex degree and highest face size is listed. Of all these maps, only the first five listed in Table 4 will attain their Platonicity by the use of single edges and are therefore further discussed. Depending on their valency they can be divided into trivalent ({7,3}, {8,3}, {12,3}) and tetravalent maps ({6,4}, {8,4}).

Let us start with the realization of trivalent maps which can be considered as blueprints for some highly symmetrical sp^2 hybridized carbon allotropes. The first member, the Klein map {7,3}, is named after the 19th century mathematician Felix Klein who investigated its very high-symmetry group (order 336) in connection with the theory of multivalued functions.[34] A Schlegel-like representation of this 56-vertex map is given in Figure 8 and can be seen to consist of 24 heptagonal faces. As the highest possible crystallographic point group of this map has O_h symmetry we chose the Plumber's nightmare as the underlying surface. This surface

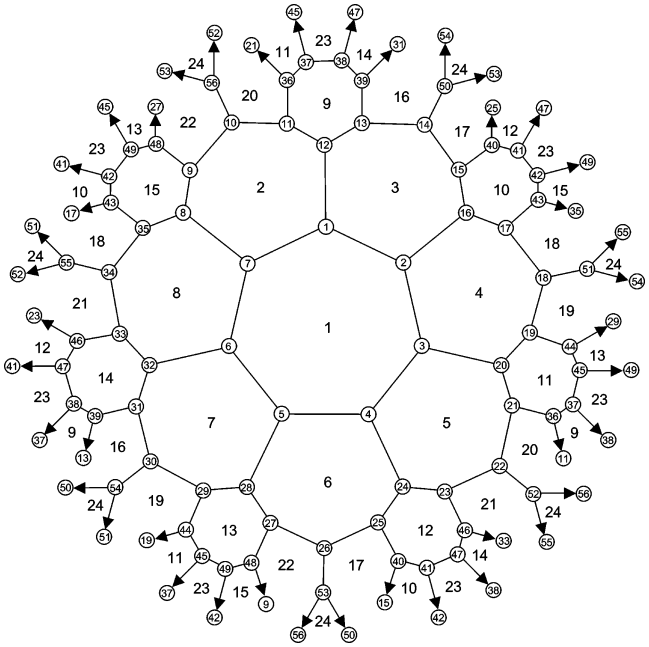

Figure 8. Schlegel-like representation for the 56 vertex Klein map consisting of 24 heptagonal faces.

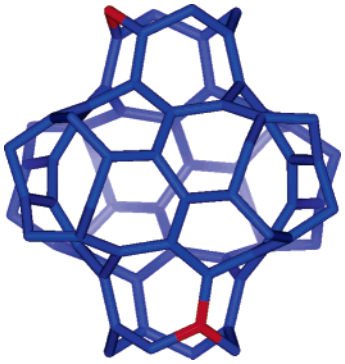

Figure 9. All-heptagon carbon network on the plumber's nightmare based on the regular Klein map. The structure is chiral and exhibits octahedral *O* symmetry. Two equivalent vertices are indicated in red and show the inherent twist of 90° between the tubes.

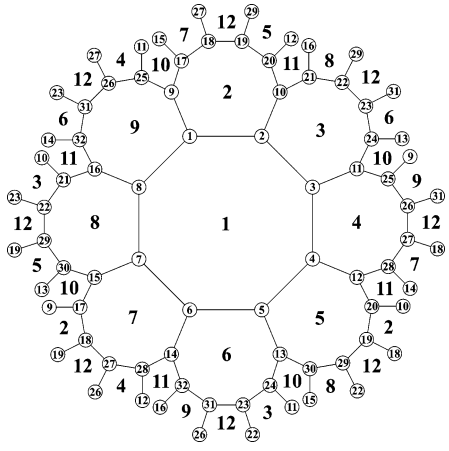

Figure 10. Schlegel-like representation for the 32 vertex Dyck map consisting of 12 octagons.

consists of 3 intersecting tubes which run along the directions of a set of Cartesian axes. Normally, one would expect a realization of this Klein map which exhibits O_h symmetry, but as the map is intrinsically chiral its highest possible realization will be only of octahedral *O* symmetry.[16] In Figure

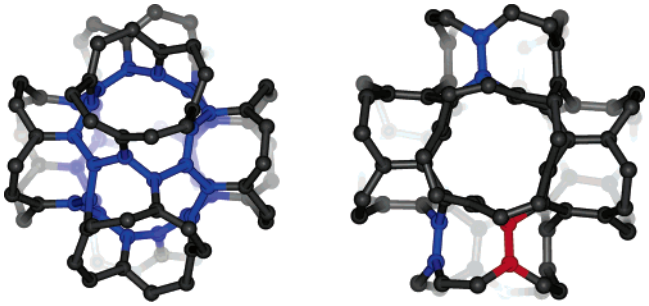

Figure 11. All-octagon carbon network on the plumber's nightmare based on the regular Dyck map. The structure is chiral and exhibits octahedral *O* symmetry. Left: Atoms and edges indicated in blue belong to the same unit-cell; all other vertices belong to neighboring unit-cells and are only included to show the octagonal faces. Right: Equivalent edges are indicated in blue and lead to a 60° twist on identification. Identification of the upper blue and lower red edge leads to the least strained structure which still incorporates a twist of 30°.

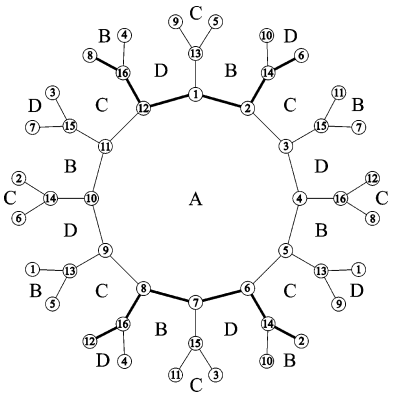

Figure 12. Schlegel-like representation of the 16 vertex genus-3 Möbius-Kantor map. One closed Petrie-path is indicated in bold lines and corresponds with face B of the genus-2 Möbius-Kantor map of Figure 4.

9 we show this molecular realization after the vertices were substituted by carbon atoms and optimized using molecular modeling (MM+). Note that the model contains 80 atoms as some vertices are exactly located on the boundaries of the tubes and therefore duplicated. These bounding vertices will play a crucial role as they determine how the different unit-cells should be glued together to form a 3D zeolite-like network. In fact, the connectivity of the original Klein map is only preserved when the tubes of neighboring unit-cells are twisted over an angle of 90° before they are glued together. This mismatch can be seen in Figure 9 where we marked two atoms which share a common vertex label. The originating strain can however be completely relaxed if we choose not to apply a twist. In this case we end up with a Klein-like structure which is also completely tessellated by heptagons but for which the connectivity does no longer correspond to that of the Klein graph. These and similar structures have been proposed as models for carbon foams.[5−7,35]

The second trivalent regular map, the Dyck map {8,3}, is slightly less symmetrical (order 192) and consists of 32 vertices and 12 octagonal faces (Figure 10). It was discovered by Walther von Dyck who was a doctoral student of Klein.[36] Exactly as for the Klein graph, it contains O_h as its highest order crystallographic group but, as it is intrinsically chiral, can only be realized with *O* symmetry.[14,15] The corresponding realization is shown in Figure 11. Notice, that only the atoms indicated in blue (Figure 11a) are part of the actual unit-cell. The remaining atoms belong to one of the neighboring unit-cells and are only included to show the octagonal faces which are divided over two neighboring cells. Once again there is a small mismatch of 60° between the tubes as can be seen in Figure 11b where we provided two equivalent edges with a blue color. The best we can do to relax the strain is to identify the upper blue edge with the lower red edge which still leads to a 30° mismatch. So contrary to the Klein map, there will always be a little bit of strain, even if we dismiss the requirement of exact Dyck-like connectivity.

The third and last trivalent regular map {12,3} has 16 vertices and contains only 4 faces of length 12. The underlying graph is the Möbius-Kantor graph which we already encountered in our discussion of the genus 2 Platonics. This reappearance is not a coincidence but results from a deep topological connection between these two maps. They are related by a different type of dualism: *Petrie dualism*.[22] A Petrie dual of a map preserves the symmetry of the map and its underlying graph but generally changes the topology and so the surface on which the graph is embedded. Given a map, the faces of its Petrie-dual can be found by tracing Petrie paths which are formed by taking alternating left and right turns on the parent map. In Figure 12 we show a Schlegel-like projection of the genus-3 Möbius-Kantor map together with one of its Petrie-paths which is indicated in bold. The chosen path exactly corresponds with the octagonal face *B* of the genus-2 Möbius-Kantor map of Figure 4. As stated before, the highest symmetry crystallographic subgroup of this Möbius-Kantor

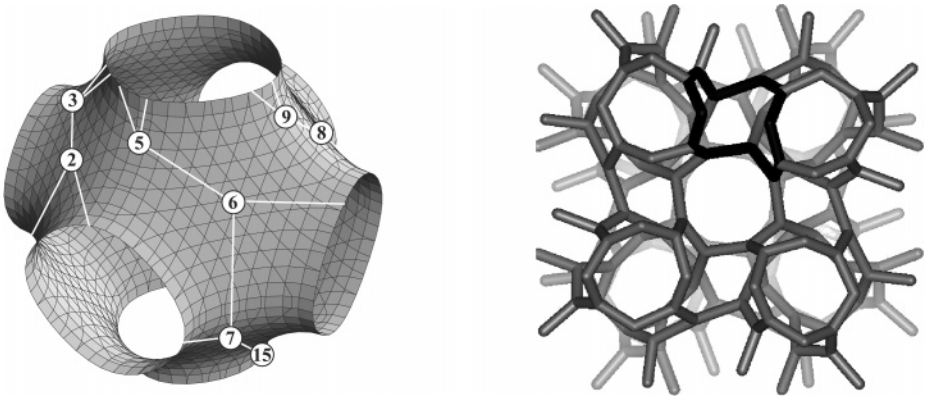

Figure 13. Left: Realization of the all-dodecagon Möbius-Kantor map on the genus-3 plumber's nightmare. Right: 2 × 2 × 2 supercell with one of the dodecagonal faces indicated in black.

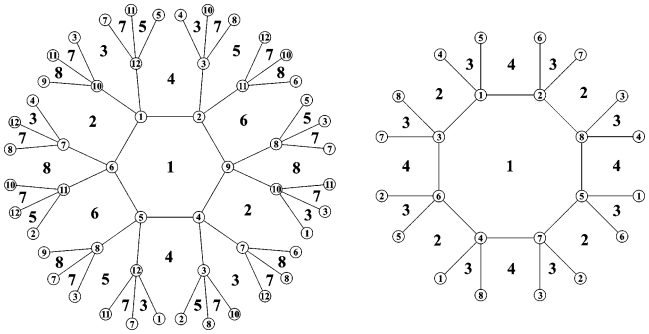

Figure 14. Schlegel-like representation of the tetravalent map {6,4} with 12 vertices and 8 hexagonal faces (left) and the tetravalent map {8,4} with 8 vertices and 4 octagonal faces (right).

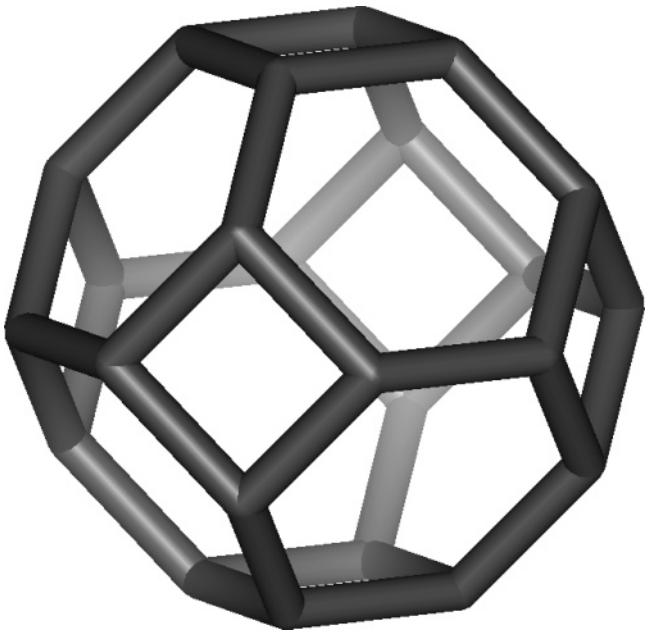

Figure 15. Spatial realization of the all-hexagon map {6,4} with O_h symmetry.

map corresponds to D_6 symmetry. However, as the D_6 point group is fully rotational, all its elements should be rotational elements of the genus-3 map. As this is not the case the possibility of a D_6 realization can be excluded, and one should turn to the second highest crystallographic subgroup, which exhibits D_4 symmetry. On the left of Figure 13 we show a pictorial representation of such a realization on the plumber's nightmare. The right-hand side of Figure 13 shows the topview of a $2 \times 2 \times 2$ supercell where one of the dodecagonal faces is indicated in black. Notice that, contrary to the Dyck and Klein map, the D_4 group is not capable of preserving the isotropy in all three spatial dimensions.

In Figure 14 we show the Schlegel-diagrams of the two regular tetravalent maps {6,4} and {8,4}. As they are not investigated in the mathematical literature they have not yet received a name, so we will just identify them by their corresponding Schläfli symbols. Their 3D realizations are shown in Figures 15 and 16. The structure of the map {6,4} is easily identified with the truncated octahedron and therefore exhibits O_h symmetry. We have chosen here not to depict the underlying plumber's nightmare surface, but it can easily be reconstructed if one thinks of the six tubes as running through the squares. The squares are thus not part of the surface which is only tessellated by hexagons. In this

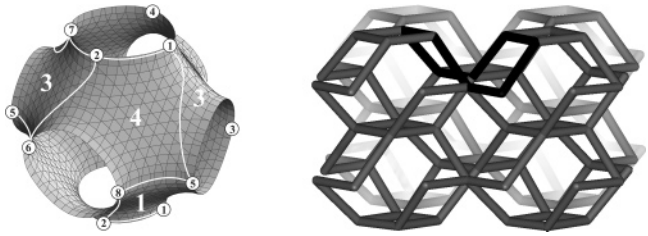

Figure 16. Left: Pictorial representation of the all-octagon map {8,4} with D_4 symmetry on the plumber's nightmare. Right: $2 \times 2 \times 2$ supercell with one of the octagonal faces indicated in black.

case, the labels of the vertices on opposite boundaries exactly match so their is no need for a twist in forming a 3D lattice. Let us note that the coordinates of Figure 15 were found by a substitution of the vertices by carbon atoms followed by an optimization of the resulting carbon four-six cage. Although this structure is trivalent, the fourth valency naturally arises when a 3D lattice is constructed. This lattice very much resembles a zeolite of type A (LTA).

The last regular map {8,4} of genus 3 only consists of 8 vertices and is tessellated by 4 octagons. Its highest crystallographic subgroup corresponds with D_{4h}. However, for a 3D realization we have to turn to the second highest subgroup which has D_4 symmetry. On the left-hand side of Figure 16 we give a pictorial representation of this all-octagon map on the plumber's nightmare. The exact locations of all 8 vertices are shown, and the placement of the edges on the forward pointing octant suffice to reconstruct the missing parts of this realization. Each octant contains exactly one-half of an octagonal face so all faces are distributed over two neighboring unit-cells. This can easily be seen on the right-hand side of Figure 16 where we present a $2 \times 2 \times 2$ supercell for this structure with one of the octagonal faces indicated in black.

7. CONCLUSIONS

The Platonic solids are all possible regular polyhedral coverings of the sphere with triangles, squares, and pentagons. As we have shown regular polyhedra with higher-order faces are possible if one considers surfaces of higher genus. From genera 1 to 3 we have found Platonic maps consisting of hexagons, heptagons, octagons, and even dodecagons. For each case we have presented molecular frameworks that correspond to building blocks of periodic lattices. So far only the simplest case of the genus-1 torus is well documented in molecules through the rich structural chemistry of the carbon nanotubes. No doubt many wonders lie ahead.

ACKNOWLEDGMENT

This work was supported by the Belgian National Science Foundation (FWO-Vlaanderen) and by the Concerted Action Scheme of the Belgian Government.

Supporting Information Available: List of coordinates (ml2-format) of the structures discussed in this paper. This material is available free of charge via the Internet at http://pubs.acs.org.

REFERENCES AND NOTES

(1) Heilbronner, E.; Dunitz, J. D. *Reflections on Symmetry: In Chemistry ... and Elsewhere*; Wiley-VCH: Weinheim, 1993.

(2) Pitochelli, A. R.; Hawthorne, F. M. The isolation of the icosahedral $B_{12}H_{12}^{2-}$ ion. *J. Am. Chem. Soc.* **1960**, *82*, 3228−3229.
(3) Ternansky, R. J.; Balogh, D. W.; Paquette, L. A. Dodecahedrane. *J. Am. Chem. Soc.* **1982**, *104*, 4503−4504.
(4) Kroto, H. W.; Heath, J. R.; O'Brien, S. C.; Curl, R. F.; Smalley, R. E. C_{60} Buckminsterfullerene. *Nature* **1985**, *318*, 162−163.
(5) King, R. B. Negative curvature surfaces in chemical structures. *J. Chem. Inf. Comput. Sci.* **1998**, *38*, 180−188.
(6) King, R. B. Platonic tessellations of Riemann surfaces as models in chemistry: Nonzero genus analogues of regular polyhedra. *J. Mol. Struct.* **2003**, *656*, 119−133.
(7) Mackay, A. L.; Terrones, H. Diamond from graphite. *Nature* **1991**, *352*, 762−762.
(8) Flapan, E. *When Topology Meets Chemistry: A Topological Look at Molecular Chirality*; Cambridge University Press: Cambridge, U.K., 2000.
(9) Klein, D. J. Topo-graphs, embeddings and molecular structure. In *Chemical Topology: Introduction and Fundamentals*; Rouvray, D. H., Bonchev, D., Eds.; Gordon and Breach Science Publishers: 1999.
(10) Siegel, J. S. Chemical topology and interlocking molecules. *Science* **2004**, *304*, 1256−1258.
(11) Cantrill, S. J.; Chichak, K. S.; Peters, A. J.; Stoddart, J. F. Nanoscale borromean rings. *Acc. Chem. Res.*, **2005**, *38*, 1−9.
(12) Lijnen, E.; Ceulemans, A. Oriented 2-cell embeddings of a graph and their symmetry classification: Generating algorithms and case study of the Möbius-Kantor graph. *J. Chem. Inf. Comput. Sci.* **2004**, *44*, 1552−1564.
(13) Ceulemans, A.; Lijnen, E. The polyhedral state of molecular matter. *Eur. J. Inorg. Chem.* **2002**, *7*, 1571−1581.
(14) Ceulemans, A.; Lijnen, E.; Ceulemans, L. J.; Fowler, P. W. The tetrakisoctahedral group of the Dyck graph and its molecular realization. *Mol. Phys.* **2004**, *102*, 1149−1163.
(15) Lijnen E.; Ceulemans, A. The symmetry of the Dyck graph: Group structure and molecular realization. In *Nanostructures − Novel Architectures*; Diudea, M., Ed.; Nova Science Publishers Inc.: Haup-page, New York: 2005.
(16) Ceulemans A.; King R. B.; Bovin, S. A.; Rogers, K. M.; Troisi A.; Fowler, P. W. The heptakisoctahedral group of the Dyck graph and its molecular realization. *J. Math. Chem.* **1999**, *26*, 101−123.
(17) Diestel, R. *Graph Theory*, 2nd ed.; Springer-Verlag: New York, 2000.
(18) Balaban, A. T. *Chemical Applications of Graph Theory*; Academic Press: London, 1976.
(19) Gross, J. L.; Tucker, T. W. *Topological Graph Theory*; Dover Publications: Mineola, NY, 2001.
(20) In this paper only orientable surfaces are considered; these are surfaces that have an inside and an outside.
(21) Conder, M.; Dobsanyi, P. Determination of all regular maps of small genus. *J. Comb. Theory B* **2001**, *81*, 224−242.
(22) McMullen, P.; Schulte, E. *Abstract Regular Polytopes*; Cambridge University Press: Cambridge, 2002.
(23) Coxeter, H. S. M. *Generators and Relations for Discrete Groups*; Springer-Verlag: Berlin, 1972.
(24) Maier, G.; Neudert, J.; Wolf, O.; Pappusch, D.; Sekiguchi, A.; Tanaka, M.; Matsuo, T. Tetrakis(trimethylsilyl)tetrahedrane. *J. Am. Chem. Soc.* **2002**, *124*, 13819−13826.
(25) Eaton, P. E.; Cole, T. W., Jr. Cubane. *J. Am. Chem. Soc.* **1966**, *86*, 3157−3158.
(26) Zhang, M. X.; Eaton, P. E.; Gilardi, R. Hepta- and octanitrocubanes. *Angew. Chem., Int. Ed.* **2000**, *39*, 401−404.
(27) Prinzbach, H.; Weiler, A.; Landenberger, P.; Wahl, F.; Wörth, J.; Scott, L. T.; Gelmont, M.; Olevano, D.; Issendorff, B. V. Gas-phase production and photoelectron spectrocopy of the smallest fullerene, C_{20}. *Nature* **2000**, *407*, 60−63.
(28) Boone, J. L. Isolation of the Hexahydroclosohexaborate(2-) anion, $B_6H_6^{2-}$. *J. Am. Chem. Soc.* **1964**, *86*, 5036−5036.
(29) Boldyrev, A. I.; Simons, J. Polyhedral ionic molecules. *J. Am. Chem. Soc.* **1997**, *119*, 4618−4621.
(30) Preetz, W.; Peters, G.; Bublitz, D. Preparation and spectroscopic investigations of mixed octahedral complexes and clusters. *Chem. Rev.* **1996**, *96*, 977−1026.
(31) Iijima, S. Helical microtubules of graphite carbon. *Nature* **1991**, *354*, 56−58.
(32) This labeling is nonunique and redundant. More rigorous labeling schemes only require three indices: Negami, S. Uniqueness and faithfulness of embedding of toroidal graphs. *Discrete Math.* **1983**, *44*, 161−180.
(33) Bovin, S. A.; Chibotaru, L. F.; Ceulemans, A. The quantum structure of carbon tori. *J. Mol. Catal. A* **2001**, *166*, 47−52.
(34) Klein, F. Über die Transformation siebenter Ordnung der elliptischen Funktionen. *Math. Ann.* **1879**, *14*, 428−471.
(35) Vanderbilt, D.; Tersoff, J. Negative curvature fullerene analogue of C_{60}. *Phys. Rev. Lett.* **1992**, *68*, 511−513.
(36) Dyck, W. Über Aufstellung und Untersuchung von Gruppe und Irrationalität regulärer Riemannscher Flächen. *Math. Ann.* **1880**, *17*, 473−509.

CI0502496